

First-principles prediction of disordering tendencies in pyrochlore oxides

Chao Jiang,* C. R. Stanek, K. E. Sickafus, and B. P. Uberuaga

Materials Science and Technology Division, Los Alamos National Laboratory, Los Alamos, New Mexico 87545, USA

(Received 17 September 2008; revised manuscript received 19 February 2009; published 18 March 2009)

Using first-principles calculations, we systematically predict the order-disorder energetics of series of zirconate ($A_2Zr_2O_7$), hafnate ($A_2Hf_2O_7$), titanate ($A_2Ti_2O_7$), and stannate ($A_2Sn_2O_7$) pyrochlores. The disordered defect-fluorite structure is modeled using an 88-atom two-sublattice special quasirandom structure (SQS) that closely reproduces the most relevant near-neighbor intrasublattice and intersublattice pair-correlation functions of the random mixture. The order-disorder transition temperatures of these pyrochlores estimated from our SQS calculations show overall good agreement with existing experiments. We confirm previous studies suggesting that the bonding in pyrochlores is not purely ionic and thus electronic effects also play a role in determining their disordering tendencies. Our results have important consequences for numerous applications, including nuclear waste forms and fast ion conductors.

DOI: 10.1103/PhysRevB.79.104203

PACS number(s): 64.60.Cn, 61.80.Az, 81.30.Dz

$A_2B_2O_7$ pyrochlores are an important class of oxide materials that are being considered for nuclear applications including the immobilization of actinides in nuclear waste¹⁻³ and inert matrix fuel.^{4,5} The pyrochlore structure (space group $Fd\bar{3}m$) is closely related to the fluorite structure (space group $Fm\bar{3}m$) and can be considered as an ordered fluorite derivative, i.e., BO_2 fluorite with half of the tetravalent B^{4+} cations replaced by trivalent A^{3+} accompanied by charge-compensating structural oxygen vacancies. Here both the cations and anions are fully ordered such that each A^{3+} (B^{4+}) cation is coordinated by eight (six) nearest-neighbor oxygen atoms. The pyrochlore structure can be transformed into the disordered defect-fluorite structure by randomly distributing the cations and anions on their respective sublattices.

As a nuclear material, the host must be highly resistant to radiation damage. This is because irradiation will create atomic scale defects, which with time will accumulate, possibly leading to amorphization and/or microcracking of the crystalline structure. The two most important atomistic defects that are created in $A_2B_2O_7$ pyrochlore oxides when exposed to displacive radiation damage conditions are cation antisite defects ($O \rightarrow A_B + B_A$) and anion Frenkel pairs ($O \rightarrow V_O + O_i$).^{6,7} Interestingly, these defects are precisely the ones that are responsible for the pyrochlore to fluorite order-disorder transformation. In other words, radiation damage inherently involves disordering processes (for example, neutron-diffraction measurements showed that the Mg and Al sublattices in $MgAl_2O_4$ spinel are fully disordered after high-fluence neutron irradiation⁸). Our earlier studies^{2,3} found that oxides that show a natural propensity to accommodate lattice disorder will be less susceptible to detrimental radiation damage effects such as amorphization. Therefore, the order-disorder phase transition under equilibrium condition is the focus of this work. An understanding of structural disorder is also important for other properties such as ionic conductivity.^{9,10}

A number of materials properties have been proposed in the literature to indicate the disordering tendencies of pyrochlores, including the formation energy of disordering point defects,^{2,7,11,12} the order-disorder transformation temperature T_{O-D} ,³ and the 48f oxygen positional parameter x .¹³ In this paper, we calculate the energy difference between the fully

ordered pyrochlore and the fully disordered defect-fluorite structures, i.e., the disordering energy $\Delta E_{\text{disorder}}$, and propose this quantity as a key indicator of radiation tolerance in complex oxides. As will be shown, the present indicator has several advantages over the previous ones. Our calculations are performed using the all-electron projector-augmented wave method within the generalized gradient approximation (GGA), as implemented in Vienna *ab initio* simulation package (VASP) code.¹⁴ The lattice parameters and internal atomic positions of all structures are fully relaxed using a conjugate-gradient scheme. According to our convergence tests, a plane-wave cutoff energy of 400 eV and a $2 \times 2 \times 2$ k -point sampling are sufficient to give fully converged results. Previous theoretical studies¹⁵⁻¹⁹ have demonstrated that GGA gives structural and electronic properties of pyrochlores in good agreement with experiments.

The special quasirandom structure (SQS) approach²⁰⁻²² is adopted to adequately reproduce the statistics of a random alloy in a small (thus computationally feasible) periodic supercell. Using the Monte-Carlo simulated annealing technique, we have developed an 88-atom SQS for the fully disordered $(A_{1/2}B_{1/2})(O_{7/8}V_{1/8})_2$ defect-fluorite structure (see Table I for detailed structural information of this SQS). As the fcc cation and simple-cubic anion sublattices do not exchange species, the configurational problem can be greatly simplified to that of a binary system.²³ Thus, the total energy of the system depends on two types of interatomic interactions: those between atoms within the same sublattice (cation-cation and anion-anion) and those between atoms on different sublattices (cation-anion). As shown in Table II, both the near-neighbor intrasublattice and intersublattice pair-correlation functions of the random defect-fluorite structure are accurately reproduced by the SQS. We note that, upon relaxation of the SQS, one of the 56 oxygen atoms exchanges position with a neighboring vacancy. However, if we compare the correlation functions of an idealized version of this relaxed structure with that of the original SQS, we find that they change by less than 0.02. This fact, combined with the good agreement we obtain with experiments in predicting T_{O-D} , as will be discussed below, leads us to conclude that the SQS approach is suitable for describing the disordered state of pyrochlores.

TABLE I. Structural description of the 88-atom SQS for mimicking the fully disordered $(A_{1/2}B_{1/2})(O_{7/8}V_{1/8})_2$ defect-fluorite structure. Lattice vectors and atomic positions are given in Cartesian coordinates, in units of a , the fluorite lattice parameter. Atomic positions are given for the ideal, unrelaxed fluorite sites.

Lattice vectors			
$a_1=(1, 1, -2), a_2=(1, 2, -1), a_3=(2, -1, 1)$			
Atomic positions of A cations			
(2.5, 0, -0.5)	(1, 0, 0)	(1.5, 1 -0.5)	(1.5, 0.5, -1)
(1, 0.5, -0.5)	(1.5, 1, -1.5)	(2.5, 1, -0.5)	(3, 1.5, -1.5)
(1, 1, -1)	(1.5, 1.5, -2)	(2, 2.5, -2.5)	(2, 0.5, -0.5)
(3.5, 1.5, -1)	(3.5, 1, -1.5)	(4, 2, -2)	(2, 1, -1)
Atomic positions of B cations			
(2, -0.5, 0.5)	(2.5, 0.5, 0)	(3, 1, -1)	(2, 1.5, -1.5)
(1.5, 1.5, -1)	(2, 2, -2)	(2, 0, 0)	(2.5, 0.5, -1)
(1.5, 2, -1.5)	(2.5, 1.5, -1)	(2.5, 1, -1.5)	(3, 2, -2)
(3, 0.5, -0.5)	(2.5, 2, -1.5)	(2.5, 1.5, -2)	(3, 2.5, -2.5)
Atomic positions of oxygen atoms			
(2.25, 0.25, -0.25)	(1.75, 0.25, -0.25)	(1.25, 0.75, -0.75)	(1.75, 1.75, -1.25)
(2.25, 2.25, -2.25)	(0.75, 0.75, -0.75)	(1.25, 1.75, -1.25)	(1.25, 1.25, -1.75)
(1.25, 1.25, -1.25)	(1.75, 2.25, -1.75)	(1.75, 1.75, -2.25)	(2.75, 0.25, -0.25)
(3.25, 1.25, -0.75)	(3.75, 1.75, -1.75)	(2.75, 1.25, -1.75)	(1.75, 0.75, -0.75)
(2.25, 1.75, -1.25)	(2.75, 2.25, -2.25)	(0.25, 0.25, -0.25)	(1.25, 1.75, -1.75)
(2.25, 0.25, 0.25)	(2.25, -0.25, -0.25)	(1.25, -0.25, 0.25)	(1.75, 0.75, -0.25)
(1.75, 0.25, -0.75)	(2.25, 1.25, -1.25)	(1.25, 0.75, -0.25)	(1.75, 1.25, -1.25)
(2.25, -0.25, 0.25)	(2.75, 0.75, -0.25)	(2.75, 0.25, -0.75)	(3.25, 1.25, -1.25)
(1.75, -0.25, 0.25)	(2.25, 0.75, -0.25)	(2.25, 0.25, -0.75)	(2.75, 1.25, -1.25)
(1.25, 0.25, -0.25)	(2.25, 1.75, -1.75)	(0.75, 0.25, -0.25)	(1.25, 1.25, -0.75)
(1.25, 0.75, -1.25)	(1.75, 1.75, -1.75)	(2.25, 0.75, -1.25)	(3.25, 0.75, -1.25)
(2.25, 0.75, -0.75)	(1.75, -0.75, 0.75)	(0.75, -0.25, 0.25)	(1.75, 0.75, -1.25)
(2.75, 0.75, -1.25)	(2.25, 1.25, -0.75)	(1.75, 1.25, -1.75)	(2.25, 2.75, -2.75)
(3.25, 2.25, -2.25)	(2.75, 0.75, -0.75)	(1.75, 1.25, -0.75)	(3.25, 1.75, -1.75)
Positions of structural oxygen vacancies			
(2.75, 1.25, -0.75)	(2.75, 1.75, -1.75)	(1.75, 2.25, -2.25)	(2.75, 1.75, -1.25)
(0.75, 1.25, -0.75)	(0.75, 0.75, -1.25)	(1.25, 0.25, -0.75)	(2.25, 1.25, -1.75)

We obtain $\Delta E_{\text{disorder}}$ as the first-principles calculated total-energy difference between the pyrochlore and the SQS. A large $\Delta E_{\text{disorder}}$ indicates that the crystalline lattice does not tolerate disorder and its internal energy will quickly increase

upon accumulation of irradiation-induced disordering point defects, giving rise to a thermodynamic driving force for the lattice to collapse into aperiodic amorphous structure.²⁴ On the contrary, a small $\Delta E_{\text{disorder}}$ indicates that the lattice sta-

TABLE II. Intrasublattice (cation-cation and anion-anion) and intersublattice (cation-anion) pair-correlation functions of the 88-atom SQS for mimicking the random fluorite $(A_{1/2}B_{1/2})(O_{7/8}V_{1/8})_2$ structure. nn=nearest neighbor.

	Cation-Cation					Anion-Anion					Cation-Anion		
	1nn	2nn	3nn	4nn	5nn	1nn	2nn	3nn	4nn	5nn	1nn	2nn	3nn
Random Alloy	0	0	0	0	0	0.5625	0.5625	0.5625	0.5625	0.5625	0	0	0
SQS	0	0	0	0	0	0.5625	0.5625	0.5625	0.5625	0.5625	0	0.005	0.005

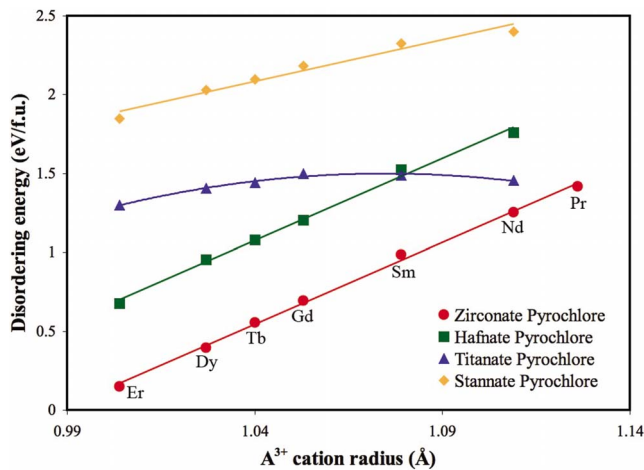


FIG. 1. (Color online) Calculated disordering energies (eV per $A_2B_2O_7$ formula unit) of pyrochlores as a function of A^{3+} cation radius. The trend lines (solid lines) are drawn to guide the eye.

bility is not much disturbed by the disordering defects and the material thus exhibits good radiation tolerance.

Figure 1 shows the calculated disordering energies of $A_2B_2O_7$ (where A^{3+} is a rare-earth element and $B^{4+} = \text{Zr, Hf, Ti, Sn}$) pyrochlores as a function of the A^{3+} cationic radius from Shannon.²⁵ For zirconate, hafnate and stannate pyrochlores, $\Delta E_{\text{disorder}}$ increases with increasing A^{3+} size in an approximately linear fashion. Such a trend is in agreement with our previous study using Born-like empirical potentials to describe ionic crystals,^{2,3} and the general view that the size difference between A^{3+} and B^{4+} cations is the driving force for ordering in the pyrochlore structure.²⁶ However, the titanate pyrochlore series is clearly an exception. Instead of monotonically increasing with A^{3+} size, the disordering energies of titanate pyrochlores actually exhibit a maximum at $\text{Gd}_2\text{Ti}_2\text{O}_7$. Interestingly, such a finding is consistent with the experimental observations by Lian *et al.*¹³ that $\text{Gd}_2\text{Ti}_2\text{O}_7$ has the highest critical amorphization temperature (above which no amorphization occurs regardless of radiation dose) among all titanate pyrochlores. It also agrees with previous studies using empirical potentials⁷ and first-principles calculations,¹⁷ showing that $\text{Gd}_2\text{Ti}_2\text{O}_7$ indeed has the largest defect formation energy among titanate pyrochlores.

Figure 1 further shows that for the same A^{3+} cation, it is more difficult to disorder stannate pyrochlores than titanate pyrochlores, which is quite surprising since the ionic radius of Sn^{4+} (0.69 Å) is much larger than that of Ti^{4+} (0.605 Å). It can also be seen that $\Delta E_{\text{disorder}}$ of a given hafnate pyrochlore is consistently larger than that of its zirconate equivalent, despite the very similar ionic radius of Zr^{4+} (0.72 Å) and Hf^{4+} (0.71 Å). Indeed, while $\text{Sm}_2\text{Zr}_2\text{O}_7$ disorders at ~ 2273 K, $\text{Sm}_2\text{Hf}_2\text{O}_7$ is stable all the way to the melt.²⁷ The T_{O-D} of $\text{Gd}_2\text{Zr}_2\text{O}_7$ is also significantly lower than that of $\text{Gd}_2\text{Hf}_2\text{O}_7$.²⁷ Clearly, such phenomena cannot be simply explained by the relative sizes of B^{4+} cations, and electronic effects must play an important role here. According to the Mulliken overlap population analysis by Lumpkin *et al.*,²⁸ the covalency of B-O bonds increases in the order $\text{Sn} > \text{Ti} > \text{Hf} > \text{Zr}$ and, as they discuss, this trend roughly follows that of Pauling's electronegativity.²⁹ Examination of elec-

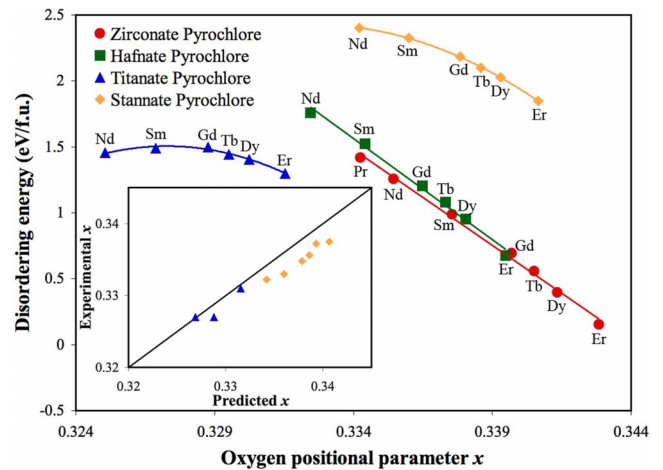


FIG. 2. (Color online) Calculated disordering energies of pyrochlores as a function of their oxygen positional parameter, x . The inset shows the comparisons between predicted and experimentally measured x values of pyrochlore oxides.

tronic structure also revealed that the Sn-O bond is substantially more covalent than Ti-O and Zr-O bonds.¹² Presumably, the strong covalent nature of Sn-O bonds may be the origin of the high phase stability of stannate pyrochlores. The fact that Hf-O bonds are more covalent than Zr-O bonds may also explain why hafnate pyrochlores are more difficult to disorder than zirconate pyrochlores.

It has been suggested that the positional parameter x of oxygen atoms occupying 48f sites in an ordered pyrochlore structure may determine its order-disorder energetics.¹³ For an ideal pyrochlore structure, $x = 0.3125$ such that each B^{4+} cation is surrounded by an ideal oxygen octahedron. The x parameter for a completely disordered defect-fluorite structure is 0.375. Figure 2 shows our calculated $\Delta E_{\text{disorder}}$ as a function of x obtained from fully relaxed pyrochlore unit cells. We find that $\Delta E_{\text{disorder}}$ decreases with increasing x within a given pyrochlore family (same B^{4+} cation) for the zirconates, hafnates, and stannates. Such a conclusion is in agreement with previous experimental studies.¹³ However, this trend does not apply to titanate pyrochlores, where $\text{Gd}_2\text{Ti}_2\text{O}_7$ has the highest $\Delta E_{\text{disorder}}$, but not the smallest x . x is also not a very good indicator of disordering propensities between different pyrochlore families. Figure 2 (inset) further shows that our predicted x values are in good agreement with available experimental data.^{30,31} Here only results for those titanate and stannate pyrochlores with a strong tendency for ordering are shown. For zirconate and hafnate pyrochlores that generally show a much weaker ordering tendency, direct comparison between experiments and theory becomes difficult since the x parameter is known to vary with the actual extent of disorder in a sample that will depend sensitively on its heat treatment history,^{32,33} though our calculated x values compare rather well with previous first-principles studies.¹⁶⁻¹⁹ While not shown, we observe that our calculated x parameters for zirconate, hafnate, titanate, and stannate pyrochlores decrease monotonically and linearly with increasing A^{3+} size, which is in agreement with our previous study.³²

Assuming ideal configurational entropy of mixing for the

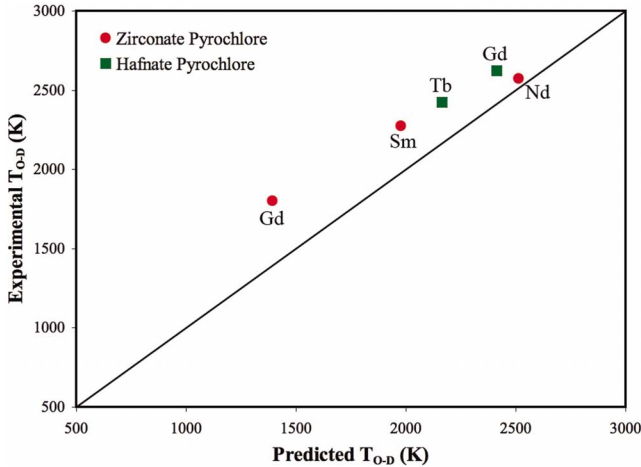


FIG. 3. (Color online) Comparisons between predicted and experimentally measured T_{O-D} 's of pyrochlores. The solid line represents perfect agreement between calculations and experiments.

disordered fluorite structure, we can estimate the pyrochlore to fluorite order-disorder temperature as $T_{O-D} \approx \Delta E_{\text{disorder}} / \Delta S_{\text{ideal}}$, where $\Delta S_{\text{ideal}} = -4k_B[x \ln x + (1-x)\ln(1-x) + 2y \ln y + 2(1-y)\ln(1-y)]$, and k_B is the Boltzmann constant. $x = 1/2$ and $y = 1/8$ are the site fractions of B cations and oxygen vacancies on their respective sublattices. Figure 3 shows our predicted T_{O-D} 's in comparison with available experimental measurements as reviewed by Refs. 34 and 35. Remarkably, the experimentally observed ranking of T_{O-D} ($\text{Gd}_2\text{Zr}_2\text{O}_7 < \text{Sm}_2\text{Zr}_2\text{O}_7 < \text{Tb}_2\text{Hf}_2\text{O}_7 < \text{Nd}_2\text{Zr}_2\text{O}_7 \approx \text{Gd}_2\text{Hf}_2\text{O}_7$) is correctly predicted by our calculations, although on average we underestimate the experimental data by ~ 250 K. This good agreement confirms the suitability of using the SQS approach to model the disordered state of pyrochlores. The remaining quantitative discrepancy may be due to experimental uncertainties, the inaccuracies of GGA, or to the neglect of nonconfigurational (vibrational, electronic, etc.) entropies in our estimations.

While not shown in Fig. 3, the T_{O-D} 's of $\text{Er}_2\text{Zr}_2\text{O}_7$, $\text{Dy}_2\text{Zr}_2\text{O}_7$, $\text{Tb}_2\text{Zr}_2\text{O}_7$, $\text{Pr}_2\text{Zr}_2\text{O}_7$, $\text{Er}_2\text{Hf}_2\text{O}_7$, $\text{Dy}_2\text{Hf}_2\text{O}_7$, $\text{Sm}_2\text{Hf}_2\text{O}_7$, and $\text{Nd}_2\text{Hf}_2\text{O}_7$ are predicted to be 303, 793, 1115, 2840, 1358, 1909, 3054, and 3525 K, respectively. For $\text{Er}_2\text{Zr}_2\text{O}_7$ and $\text{Dy}_2\text{Zr}_2\text{O}_7$, their T_{O-D} 's are so low that the formation of ordered pyrochlore structure is prohibited due to sluggish kinetics. This explains why no ordered pyrochlore structure has been experimentally observed for these two compounds (rather, a defect-fluorite structure is observed).^{2,27} For $\text{Pr}_2\text{Zr}_2\text{O}_7$, $\text{Sm}_2\text{Hf}_2\text{O}_7$, and $\text{Nd}_2\text{Hf}_2\text{O}_7$, the predicted T_{O-D} 's are actually higher than their respective melting temperatures, consistent with the fact that these compounds do not disorder up to their melting points.²⁷ By heat treating mixtures of HfO_2 and rare-earth oxides at various annealing temperatures from 1200 up to 1700 °C, Mandal *et al.*³⁶ successfully synthesized various hafnate pyrochlores. Importantly, they found that $\text{Er}_2\text{Hf}_2\text{O}_7$ crystallizes in a defect-fluorite structure while $\text{Dy}_2\text{Hf}_2\text{O}_7$ exhibits a weakly ordered pyrochlore structure. Such experimental results are fully consistent with the present calculations since the maximum annealing temperature in those experiments is much higher than the predicted T_{O-D} of $\text{Er}_2\text{Hf}_2\text{O}_7$, but is very close

to that of $\text{Dy}_2\text{Hf}_2\text{O}_7$. Furthermore, the experimentally observed x parameter of $\text{Dy}_2\text{Hf}_2\text{O}_7$ [0.348 (Ref. 36)] is much larger than our predicted value (0.338) for the fully ordered $\text{Dy}_2\text{Hf}_2\text{O}_7$ pyrochlore, which is due to the existence of structural disorder under the experimental conditions.

Kennedy *et al.*³⁰ synthesized a wide range of stannate pyrochlores through solid-state reaction between SnO_2 and appropriate rare-earth oxides at relatively high temperatures between 1400–1500 °C. Interestingly, they found that none of those compounds exhibits any level of structural disorder within the cation or anion sublattice, indicating a strong ordering tendency of stannate pyrochlores. Furthermore, experimental $\text{TiO}_2\text{-A}_2\text{O}_3$ phase diagrams³⁷ indicate that the ordered $\text{A}_2\text{Ti}_2\text{O}_7$ pyrochlore phase is stable to the melt for the entire rare-earth (A) series. These experimental results are fully consistent with our predicted high disordering energies of stannate and titanate pyrochlores. Of all the pyrochlore oxides considered in this study, $\text{Er}_2\text{Zr}_2\text{O}_7$, $\text{Dy}_2\text{Zr}_2\text{O}_7$, and $\text{Gd}_2\text{Zr}_2\text{O}_7$ are among those with the lowest T_{O-D} 's (thus highest-disordering tendencies), in accordance with their excellent amorphization resistance.^{2,3,38} In contrast, the strongly ordered nature of stannate and titanate pyrochlores suggests that these compounds can be readily amorphized by ion irradiation. We note that, while titanate pyrochlores are generally susceptible to radiation-induced amorphization,¹³ it has been observed that $\text{Er}_2\text{Sn}_2\text{O}_7$ cannot be amorphized even at 25 K.³⁹ We are currently investigating the origins of this discrepancy.

To conclude, we have performed a systematic first-principles study of the tendency for disorder in a wide range of pyrochlores. A number of materials properties have been proposed before to indicate this tendency: the defect formation energy, the order-disorder temperature T_{O-D} , and the oxygen parameter x . We introduce the disordering energy—the energy cost required to fully disorder a pyrochlore into fluorite—as another important indicator of disordering tendency. Clearly, all of these concepts are related as they measure, in one way or another, the stability of the pyrochlore structure. However, there are several advantages associated with using the disordering energy. First, there exists a direct quantitative relationship between the disordering energy and T_{O-D} , the most direct measure of disordering tendency. However, as T_{O-D} is not always experimentally accessible—due to kinetic limitations for materials with low T_{O-D} and the preference for melting for those with high T_{O-D} —the disordering energy is more generally useful for comparing different pyrochlores. Our predicted T_{O-D} 's can also be used to complement existing phase diagrams when such information is lacking. In contrast, there exists no quantitative correlation between defect formation energy and T_{O-D} . Second, while the oxygen parameter x has been demonstrated to give some indication of disordering tendencies within a given pyrochlore family, its usefulness is limited as it is less reliable as an indicator of disordering tendency between different pyrochlore families. There are also experimental issues in measuring x , as a fully ordered pyrochlore may be difficult to achieve, especially for pyrochlores with a low T_{O-D} , where the measured value of x will depend on the degree of residual disorder that depends on sample preparation. Finally, the concept of disordering energy can be easily applied to assess

the disordering tendencies of other oxides with complex low-symmetry crystal structures such as the $A_4B_3O_{12}$ δ phase, where a unique x parameter cannot be defined and the definition of defect formation energy becomes ambiguous due to the multitude of inequivalent crystallographic sites.

This work is sponsored by the U.S. Department of Energy (DOE), Office of Basic Energy Sciences (BES), Division of Materials Sciences and Engineering. All calculations are performed using the parallel computing facilities at Los Alamos National Laboratory.

*chao@lanl.gov

- ¹S. X. Wang, B. D. Begg, L. M. Wang, R. C. Ewing, W. J. Weber, and K. V. G. Kutty, *J. Mater. Res.* **14**, 4470 (1999).
- ²K. E. Sickafus, L. Minervini, R. W. Grimes, J. A. Valdez, M. Ishimaru, F. Li, K. J. McClellan, and T. Hartmann, *Science* **289**, 748 (2000).
- ³K. E. Sickafus, R. W. Grimes, J. A. Valdez, A. Cleave, M. Tang, M. Ishimaru, S. M. Corish, C. R. Stanek, and B. P. Uberuaga, *Nat. Mater.* **6**, 217 (2007).
- ⁴S. Lutique, R. J. M. Konings, V. V. Rondinella, J. Somers, and T. Wiss, *J. Alloys Compd.* **352**, 1 (2003).
- ⁵S. J. Yates, P. Xu, J. Wang, J. S. Tulenko, and J. C. Nino, *J. Nucl. Mater.* **362**, 336 (2007).
- ⁶P. J. Wilde and C. R. A. Catlow, *Solid State Ionics* **112**, 173 (1998).
- ⁷L. Minervini, R. W. Grimes, and K. E. Sickafus, *J. Am. Ceram. Soc.* **83**, 1873 (2000).
- ⁸K. E. Sickafus, A. C. Larson, N. Yu, M. Nastasi, G. W. Hollenberg, F. A. Garner, and R. C. Bradt, *J. Nucl. Mater.* **219**, 128 (1995).
- ⁹H. L. Tuller, *J. Phys. Chem. Solids* **55**, 1393 (1994).
- ¹⁰C. Heremans, B. J. Wuensch, J. K. Stalick, and E. Prince, *J. Solid State Chem.* **117**, 108 (1995).
- ¹¹A. Chartier, C. Meis, W. J. Weber, and L. R. Corrales, *Phys. Rev. B* **65**, 134116 (2002).
- ¹²W. R. Panero, L. P. Stixrude, and R. C. Ewing, *Phys. Rev. B* **70**, 054110 (2004).
- ¹³J. Lian, J. Chen, L. M. Wang, R. C. Ewing, J. M. Farmer, L. A. Boatner, and K. B. Helean, *Phys. Rev. B* **68**, 134107 (2003).
- ¹⁴G. Kresse and J. Furthmuller, *Phys. Rev. B* **54**, 11169 (1996).
- ¹⁵R. Terki, H. Feraoun, G. Bertrand, and H. Aourag, *J. Appl. Phys.* **96**, 6482 (2004).
- ¹⁶N. Li, H. Y. Xiao, X. T. Zu, L. M. Wang, R. C. Ewing, J. Lian, and F. Gao, *J. Appl. Phys.* **102**, 063704 (2007).
- ¹⁷H. Y. Xiao, L. M. Wang, X. T. Zu, J. Lian, and R. C. Ewing, *J. Phys.: Condens. Matter* **19**, 346203 (2007).
- ¹⁸Z. J. Chen, H. Y. Xiao, X. T. Zu, L. M. Wang, F. Gao, J. Lian, and R. C. Ewing, *Comput. Mater. Sci.* **42**, 653 (2008).
- ¹⁹X. T. Zu, N. Li, and F. Gao, *J. Appl. Phys.* **104**, 043517 (2008).
- ²⁰A. Zunger, S. H. Wei, L. G. Ferreira, and J. E. Bernard, *Phys. Rev. Lett.* **65**, 353 (1990).
- ²¹S. H. Wei, L. G. Ferreira, J. E. Bernard, and A. Zunger, *Phys. Rev. B* **42**, 9622 (1990).
- ²²C. Jiang, C. Wolverton, J. Sofo, L. Q. Chen, and Z. K. Liu, *Phys. Rev. B* **69**, 214202 (2004).
- ²³P. D. Tepeš, G. D. Garbulsky, and G. Ceder, *Phys. Rev. Lett.* **74**, 2272 (1995).
- ²⁴M. Nastasi and J. W. Mayer, *Mater. Sci. Rep.* **6**, 1 (1991).
- ²⁵R. D. Shannon, *Acta Crystallogr., Sect. A: Cryst. Phys., Diff., Theor. Gen. Crystallogr.* **32**, 751 (1976).
- ²⁶B. J. Wuensch and K. W. Eberman, *JOM* **52**, 19 (2000).
- ²⁷E. R. Andrievskaya, *J. Eur. Ceram. Soc.* **28**, 2363 (2008).
- ²⁸G. R. Lumpkin, M. Pruneda, S. Rios, K. L. Smith, K. Trachenko, K. R. Whittle, and N. J. Zaluzec, *J. Solid State Chem.* **180**, 1512 (2007).
- ²⁹The electronegativity of Sn (1.96) is much larger than that of Ti (1.54), which is in turn larger than those of Hf (1.3) and Zr (1.33).
- ³⁰B. J. Kennedy, B. A. Hunter, and C. J. Howard, *J. Solid State Chem.* **130**, 58 (1997).
- ³¹Y. Tabira, R. L. Withers, L. Minervini, and R. W. Grimes, *J. Solid State Chem.* **153**, 16 (2000).
- ³²L. Minervini, R. W. Grimes, Y. Tabira, R. L. Withers, and K. E. Sickafus, *Philos. Mag. A* **82**, 123 (2002).
- ³³While x is sensitive to disorder, some properties such as lattice parameter are not and comparisons between theory and experiment are still meaningful in such cases.
- ³⁴C. R. Stanek and R. W. Grimes, *J. Am. Ceram. Soc.* **85**, 2139 (2002).
- ³⁵M. J. D. Rushton, R. W. Grimes, C. R. Stanek, and S. Owens, *J. Mater. Res.* **19**, 1603 (2004).
- ³⁶B. P. Mandal, N. Garg, S. M. Sharma, and A. K. Tyagi, *J. Solid State Chem.* **179**, 1990 (2006).
- ³⁷E. M. Levin, C. R. Robbins, and H. F. McMurdie, *Phase Diagrams for Ceramists* (American Ceramic Society, Columbus, 1964).
- ³⁸J. Lian, X. T. Zu, K. V. G. Kutty, J. Chen, L. M. Wang, and R. C. Ewing, *Phys. Rev. B* **66**, 054108 (2002).
- ³⁹J. Lian, K. B. Helean, B. J. Kennedy, L. M. Wang, A. Navrotsky, and R. C. Ewing, *J. Phys. Chem. B* **110**, 2343 (2006).